

The Return of the Proplyds - Understanding the Dynamics of Ionization Triggered Stars

Matthias Gritschneider^{1*}, Andreas Burkert^{2,3}

¹ *Astronomy and Astrophysics Department, University of California, Santa Cruz, CA 95064, USA*

² *University Observatory Munich, Scheinerstrasse 1, 81679 Munich, Germany*

³ *Max-Planck-Fellow, Max-Planck-Institute for Extraterrestrial Physics, Giessenbachstrasse 1, 85758 Garching, Germany*

19 April 2018

ABSTRACT

Proplyds and stars inside HII-regions are a well studied phenomenon. It is possible that they were triggered by the expansion of the HII-region itself. Here, we present calculations on the dynamics of HII-regions. We show that the triggered stars that form in the expanding shell of swept up material around the HII region rarely return into the HII regions on timescales that are inferred for the proplyds and observed young stars. However, in very dense environments like Orion, the triggered stars return in time. Thus, our model can explain why proplyds are barely observed in other HII regions. We propose that the properties of young stellar objects in HII regions in general depend critically on the distance from the massive, ionizing central star cluster. Closest in, there are proplyds, where the disk of a young star interacts directly with the feedback of the massive star. Further out are Class II protostars, where the ionization already removed the envelope. Even further away, one should find Class I stars, which either have been triggered by the ionizing radiation or pre-existed and have not lost their envelope yet. This radial sequence is not necessarily an age sequence but rather a result of the dwindling importance of stellar winds and ionizing radiation with distance. We investigate the observational signature of triggered star formation and find that the stellar distribution for ionization triggered star formation shows a distinct feature, a peak at the current position of the ionization front. Therefore, it is generally possible to tell triggered and in situ distributions of stars apart.

Key words: (ISM:) H II regions, ISM: globules, ISM: kinematics and dynamics, stars: formation, stars: kinematics, methods: analytical

1 INTRODUCTION

HII-regions and their constituents have been at the forefront of astronomic research for a long time (e.g. Strömgren 1939; Elmegreen & Lada 1977; Spitzer 1978). As they are bright, they lend themselves easily to observations. Within them, a host of different objects are observed, ranging from giant pillars (Hester et al. 1996) and peculiar gaseous structures to faint, evaporating globules. In the era of the Spitzer Space Telescope, a vast number of young stellar objects (YSOs) are discovered in and around them. Generally, the morphology and idealized evolution of HII regions are well understood (e.g. Strömgren 1939; Spitzer 1978). The location of YSOs in HII regions provide important information on their origin. However, up to now, little attention has been given to the question of how the YSOs have reached their

current location. Here, we attempt an analytic approach to investigate the heritage of the YSOs.

Among the YSOs, the so-called proplyds (Laques & Vidal 1979; O’Dell et al. 1993, short for protoplanetary disk) are particularly interesting. These are young protostellar disks, illuminated by an O-star in direct proximity. They are mainly found in Orion. Due to their relative proximity, their ionized envelopes and their disks can be observed in the optical with the Hubble Space Telescope (e.g. O’Dell et al. 1993; Bally et al. 2005; De Marco et al. 2006). All of those objects close to the Trapezium Cluster show near-IR counterparts (Meaburn 1988; Smith et al. 2005), indicative of star formation. O’Dell (1998) finds a weak correlation of proplyd size with the distance to the ionizing source in Orion.

Still, they are barely found in other HII-regions than Orion. This can be explained if they are extremely transient objects. Smith et al. (2005) show that the proplyds are very concentrated around the youngest ionization sources and

* E-mail: gritschn@ucolick.org

have ages less than 500 kyr. They already concluded that further out, only the remnants of proplyds, e.g. stars with very light disks are observed. Here, we test this scenario further with dynamical considerations.

Recent studies find a host of proplyd like features in various HII-regions (e.g. Smith et al. 2003 in the Carina Nebula and Wright et al. 2012 in Cygnus, further away from the ionizing source). However, nearly all of them have no IR-counterparts. It remains to be seen if they are failed proplyds or are at an earlier stage, leading to proplyd formation. Estimations of the photo-evaporation efficiency support the former assumption (e.g. Henney & O'Dell 1999).

Detailed simulations of the formation and evolution of proplyds exist (e.g. Störzer & Hollenbach 1999; García-Arredondo et al. 2001; Henney et al. 2009). However, a complete picture of their dynamics is still missing. An interesting question is whether they formed from stars triggered at the edge of the HII region that later on returned into the region, either by falling behind the expanding shell or by turning around due to gravity.

Here, we focus on the dynamical aspect, the rather straightforward question how a system of YSOs that were triggered to form in the expanding shell surrounding an HII region evolves and where these young stars during and after their proplyd phase would be found observationally. We review the basic equations in §2 and present a calculation of representative trajectories in §3. In §4 we investigate the question how big a observed sample has to be to allow for distinguishing different origins and in §5 we draw the conclusions.

2 BASIC EQUATIONS

When a massive star ionizes its surrounding, the photoionization leads to a heating of the gas. The radius of a sphere which can be immediately ionized by a source with a flux of Lyman photons J_{Ly} is given by the Strömngren radius

$$R_S = \left(\frac{3J_{\text{Ly}}}{4\pi n_0^2 \alpha_B} \right)^{1/3}, \quad (1)$$

where n_0 is the number density of the ionized gas and α_B is the recombination coefficient. Scattering between the photoelectrons and the ions and cooling processes results in an equilibrium temperature T_{ion} inside the sphere. Due to the increased pressure inside, the HII region expands into the cold surrounding. In a medium of constant density the radius at a given time t is given as

$$R_f(t) = R_s \left(1 + \frac{7}{4} \frac{c_{s,\text{hot}}}{R_s} (t - t_0) \right)^{\frac{4}{7}}, \quad (2)$$

where $c_{s,\text{hot}}$ is the sound speed of the hot, ionized gas. The velocity of the shell at a time t is

$$v_f(t) = c_{s,\text{hot}} \left(1 + \frac{7}{4} \frac{c_{s,\text{hot}}}{R_s} (t - t_0) \right)^{-\frac{3}{7}} \quad (3)$$

and the density inside the shell is

$$\rho_{\text{ion}}(t) = \rho_0 \left(1 + \frac{7}{4} \frac{c_{s,\text{hot}}}{R_s} (t - t_0) \right)^{-\frac{2}{7}}, \quad (4)$$

where ρ_0 is the initial, constant density. Here, t_0 is the time when the gas starts to react to the increase in tempera-

ture and therefore pressure and starts expanding. It can be approximated by the crossing time in the HII region, $t_0 = R_S/c_{s,\text{hot}}$.

We assume that stars form in the shell at a given time t_{SF} . Thus, the stars inherit the position and velocity of the shock front at that time. After formation they decouple from the gas and begin to move ballistically. Then, the stars are only going to be influenced by the gravitational potential which is given for the gas component by

$$V(r, t) = \frac{2}{3} \pi G \rho (r(t)^2 - 3r_{\text{max}}^2) \quad (5)$$

inside a spherically symmetric system. Here, r_{max} is the maximal radius of the potential, which is the extend of the cloud and ρ is the mean density inside r . Stars moving in the potential therefore are subject to an acceleration

$$a_{\text{spherical}}(t) = -\nabla V(r) = -\frac{4}{3} \pi G \rho r(t). \quad (6)$$

The most important point in our model is that for stars inside the ionization and shock front $\rho = \rho_{\text{ion}}(t)$, whereas for stars outside of the front $\rho = \rho_0$. Thus, the stars inside the HII-region feel less gravitational drag than the stars outside of it. If there is additional mass close to the centre, i.e. a stellar cluster of mass M_{central} associated with the ionization source, the resulting acceleration is

$$a_{\text{tot}}(t) = a_{\text{spherical}}(t) + a_{\text{central}}(t) = -\frac{4}{3} \pi G \rho r(t) - \frac{GM_{\text{central}}}{r(t)^2}. \quad (7)$$

3 TRAJECTORIES

With these basic equations we can now calculate the trajectories of the stars forming in the shell. From a given initial flux, J_{Ly} , and number density, n_0 , we derive position and velocity of the front as well as the density inside the HII-region according to Eqns 2-4. For a star formed at a time t_{SF} , this provides the initial conditions

$$r_0 = R_f(t_{\text{SF}}) \quad (8)$$

$$v_0 = v_f(t_{\text{SF}}). \quad (9)$$

We then calculate the quantities at a given time $t_i = t_{\text{SF}} + i\Delta t$ via

$$r_i = r_{i-1} + v_{i-1} \Delta t \quad (10)$$

$$a_i = -\frac{4}{3} \pi G \rho r_{i-1} - \frac{GM_{\text{central}}}{r_{i-1}^2} \quad (11)$$

$$v_i = v_{i-1} + a_i \Delta t \quad (12)$$

(see Equation 7).

We investigate three different fluxes, corresponding to a single B-star, a single O-star and an O/B-association ($J_{\text{Ly}} = 10^{48} \gamma \text{s}^{-1}$, $J_{\text{Ly}} = 10^{49} \gamma \text{s}^{-1}$ and $J_{\text{Ly}} = 10^{50} \gamma \text{s}^{-1}$). The number densities are $n_0 = 10^3 \text{ cm}^{-3}$, $n_0 = 5 \times 10^3 \text{ cm}^{-3}$ and $n_0 = 10^4 \text{ cm}^{-3}$, respectively. For simplicity, the gas is assumed to be atomic ($\mu = 1$). We use the Cloudy code to estimate the initial T_{ion} and R_S . Calculations were performed with version 08.00 of Cloudy, last described by Ferland et al. (1998). As the calculation of the trajectories is very expensive, very small time steps can be used for integration in order to minimize numerical errors due to the discretization. A resolution study shows that $\Delta t = 1 \text{ yr}$ leads to converged orbital evolution that is independent of Δt .

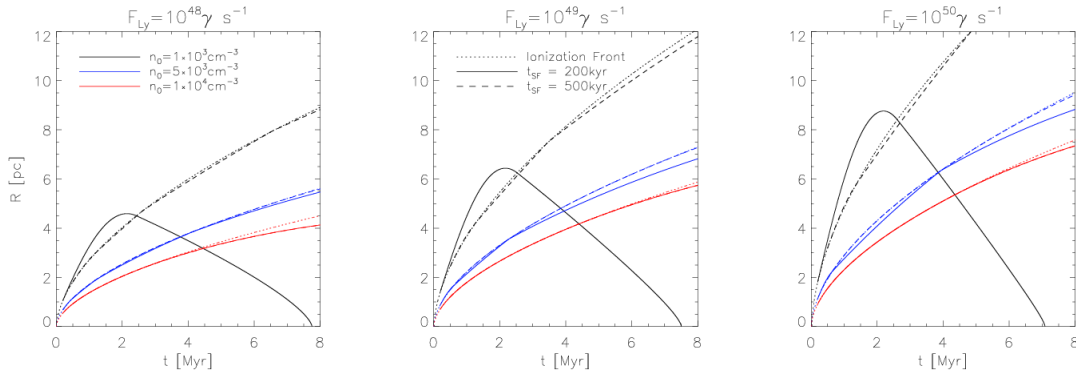


Figure 1. Trajectories of stars formed inside the ionization shock front at different times with different initial densities and fluxes. Dotted black lines show the evolution of the ionisation front. Solid and dashed lines correspond to the orbits of stars that formed after 200 kyr and 500 kyr, respectively. The stars move under the influence of the gravitational force of the gas and a central cluster of $M_{\text{central}} = 100 M_{\odot}$.

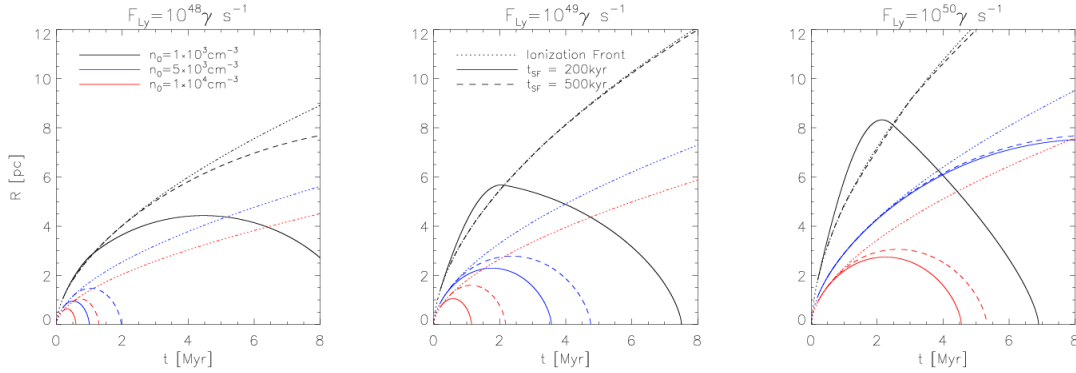


Figure 2. Same as Figure 1, but for $M_{\text{central}} = 1000 M_{\odot}$.

Case	Flux [γs^{-1}]	n_0 [cm^{-3}]	T_{ion} [K]	R_S [pc]
1A	10^{48}	1×10^3	6500	0.21
1B		5×10^3	7500	0.065
1C		1×10^4	7750	0.038
2A	10^{49}	1×10^3	7500	0.39
2B		5×10^3	8500	0.11
2C		1×10^4	8750	0.065
3A	10^{50}	1×10^3	8500	0.69
3B		5×10^3	9500	0.19
3C		1×10^4	9750	0.11

Table 1. Initial conditions for the different cases as calculated with Cloudy (Ferland et al. 1998).

The model parameters for the three cases are given in Table 1. A return of the proplyds or the stars is more likely the earlier they are formed as they are still closer to the central potential. Therefore, we investigate star formation times $t_{\text{SF}} = 200$ kyr and $t_{\text{SF}} = 500$ kyr, as suggested from simulations (e.g. Gritschneder et al. 2009).

The results are presented in Figure 1 and Figure 2 for a central mass of $M_{\text{central}} = 100 M_{\odot}$ and $M_{\text{central}} = 1000 M_{\odot}$,

respectively. Let us first focus on Figure 1. Plotted is the position of the ionization front (dotted) as well as the trajectories for stars forming after 200 kyr (solid) and 500 kyr (dashed). In all cases, the stars will overtake the ionized shell due to the fact that the shell decelerates by sweeping up the surrounding material while the stars feel just the gravitational force of the hot interior. The stars, once outside of the shell experience a stronger gravitational force by the high mass of the shell and are pulled inwards again (e.g. the black line in the middle panel of Figure 1). In the cases with higher density, the time spent outside the shell is very brief as the total mass is higher and therefore the pull inwards is stronger when the mass of the shell is added. These short ‘excursions’ beyond the shock front can lead to rather abrupt changes in the trajectory (e.g. the blue line in the right panel of Figure 1). As it can directly be seen in Figure 1, the cases the stars do not return in time to the center in order to fit the age of the proplyds. In fact they do not even return within the first ≈ 5 Myr. After that time, the first supernovae will explode, altering the system significantly¹.

With an increased central mass (Figure 2), the situa-

¹ Note that Wright et al. (2012) find proplyd-like objects at a distance of 6 – 14 pc of about 65 O-type stars in Cygnus. This could be explained by the high flux scenario (right panel of Fig-

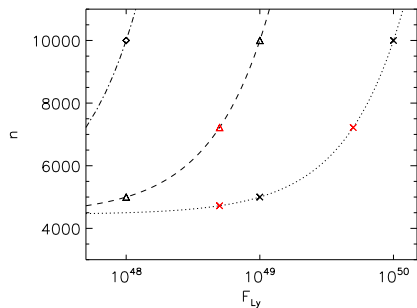


Figure 3. Flux versus density for three different groups of return times, adopting a central cluster mass of $1000 M_{\odot}$. Diamond/dash-dot: 0.5 – 1 Myr, triangles/dashed: 1 – 2 Myr and crosses/dotted: 2 – 5 Myr. Black symbols are the results from Figure 2, red symbols are additional test to assess the predictive power of this figure.

tion changes. Focussing first on the left panel of Figure 2, one can see that stars triggered in such a dense and massive stellar environment can indeed turn around within 5 Myr. However, this situation is quite unrealistic as the adapted flux is only $10^{48} \gamma s^{-1}$, whereas for central stellar masses of $1000 M_{\odot}$ there should be at least one O-star, i.e. at least a flux of $10^{49} \gamma s^{-1}$. This is the situation in the middle panel of Figure 2. Here, in the densest cases the stars return within 1 – 2 Myr, a long time before the first supernova explodes. However, those stars would still be 0.8 – 1.5 Myr old, older than the proplyds are assumed to be (< 0.5 Myr, e.g. Smith et al. 2005). As shown in the right panel of Figure 2, the situation becomes worse for even larger fluxes. However, in a very dense environment (e.g. Orion), the return time can be small enough (see below, §5).

In order to generalize our results, we divide the trajectories for the $M_{\text{central}} = 1000 M_{\odot}$ case into groups with a return time of 0.5–1 Myr, 1–2 Myr and 2–5 Myr, respectively. We plot the flux versus the density for these cases in Figure 3 and fit linearly for each age group. This figure directly allows to estimate the return time for a given observed object. In these cases the fits are $n = 4 \times 10^3 [\text{cm}^{-3}] + b \cdot F_{\text{Ly}} [\text{cm}^{-3} \text{s} \gamma^{-1}]$ with the slope being $b = 5.5 \times 10^{-45}$, $b = 5.5 \times 10^{-46}$ and $b = 5.5 \times 10^{-47}$, respectively. Remarkably, a change of return time simply means changing the slope by an order of magnitude. In order to test the predictive power, we perform additional calculations at $F_{\text{Ly}} = 5 \times 10^{48} \gamma s^{-1}$ and $F_{\text{Ly}} = 5 \times 10^{49} \gamma s^{-1}$ at the respective densities given by the fit. The resulting trajectories confirm a return in the expected time frame.

Altogether, our calculations show that triggered stars only return within the first few Myr in the densest cases. Thus, it can be readily explained that, if the proplyds have a triggered origin, they only exist in a very dense subgroup of HII regions, e.g. in Orion (see §5).

Case	A0	A1	A2	A3	A4
In situ	0.041	0.29	0.56	-0.87	0.031
Triggered	0.065	-1.5	9.1	-17.4	10.7

Table 2. Coefficients for 4th order polynomials fitted to the distributions in Fig 4, right hand panel. The distributions were normalized to the maximum value of the triggered case for the fit.

4 OBSERVABILITY

With the calculated trajectories, we can now investigate how an ensemble of triggered stars differs from a randomly in situ formed generation of stars. For reasons of simplicity, we assume stars are formed at a constant rate from 200 kyr to 500 kyr. We adopt 900 particles or stars, about the order of magnitude of stars in the Central Orion Nebula. For the in situ distribution, we adopt the most simple case that the stars are formed at a random location within $R = r_{\text{max}} = 1.5$ pc and have a randomly orientated velocity of 1 km s^{-1} . Then their position is evolved according to Eqns 10. As the total stellar mass is only a small fraction of the gas mass, we neglect their own self-gravity².

For the triggered case, we assume the stars form at a random position inside the current shock front and are subsequently subject to the same potential as in the in situ case. In the following, we focus on Case 2B. Here, there is about $6000 M_{\odot}$ swept up in the shell and $R = r_{\text{max}} = 1.5$ pc. Assuming a star formation efficiency of either 3% or 9% and every star formed having either $0.2 M_{\odot}$ or $0.6 M_{\odot}$, this would correspond to 900 stars formed, in agreement with the number of points chosen. The results at $t = 500$ kyr are shown in Figure 4 in a two-dimensional projection. The blue crosses indicate the in situ case, and the red crosses the star formation being triggered in a shell. In the right hand panel we show the distribution in radial bins and we overplot the distribution for a random distribution of stars in green in the right hand panel.

From Figure 4 the distinction is very clear. The ring-like structure in the red crosses in panel two is a clear feature of star formation, triggered in a shell-like environment. Therefore it appears possible to distinguish between a distribution of stars that was triggered compared to one that formed randomly as long as enough stars are found. The ring is the result of the relatively similar initial velocities of the stars formed in the shell during the first 500 kyr. In general, however, it is very likely that there is a mix of both populations in all observed regions.

In principle, the distribution peak of the triggered component makes it possible to distinguish triggered stars from randomly formed stars. Therefore, the two components can be told apart, at least by number. We provide the coefficients for a 4th order polynomial in Table 2.

ures 1 and 2). However, this still requires these objects to be older than 1 – 2 Myr.

² Note that the reduced gravitational potential for particles inside the HII-region is still taken into account.

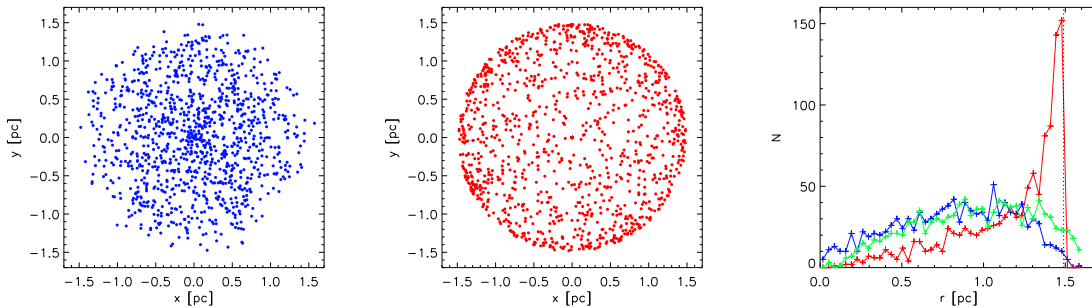


Figure 4. Left panel: Distribution of stars (random points) for a homogeneous sphere. Middle panel: distribution for a triggered shell. Right panel: comparison in radial bins. Blue: in situ, red: triggered stars. In the right hand panel a random distribution is over-plotted in green for comparison. The realizations are done for 900 points (stars). The triggered distribution has a distinct peak at the current position of the shock front (dashed line).

5 ORION

As Orion is a very dense HII-region, it is worthwhile to investigate that case in particular. The brightest star in the trapezium cluster, θ Orionis C has a luminosity of $\approx 10^{5.4} L_{\odot}$, a surface temperature of ≈ 45000 K and an age of less than 0.6 Myr (Howarth & Prinja 1989; Donati et al. 2002). For our model, we adopt these values and assume the O-star has an age of 0.6 Myr, which corresponds to the age of this subgroup (Brown et al. 1994). To estimate the density at the onset of ionization we use the current electron density in the outskirts of Orion, where the gas is less perturbed by e.g. stellar winds. From Rubin et al. (2011), we take the current value to be about 350 cm^{-3} . Running a cloudy model with an initial density of $n_0 = 4 \times 10^4 \text{ cm}^{-3}$ and the stellar values above yields a similar density after ≈ 0.6 Myr. The resulting initial conditions are $R_S = 0.025$ pc and $T_{\text{ion}} = 10^4$ K. Note that these initial conditions are out of the range of Figure 3 and in the region for short expected return times. The total stellar mass in Orion can be estimated as $384 M_{\odot}$ (e.g. Hillenbrand 1997). We calculate the trajectories for these values and plot them in Figure 5 (left hand panel). It is immediately clear, that a large number of stars are on their way inwards or in close proximity to the trapezium cluster, even after 0.6 Myr (blue dashed line). An interesting feature is the reflection point at about 0.55 Myr. Here, the first returning stars have their closest encounter with the central potential. From then on the population is mixed and there are proplyds moving inwards and outwards. In the middle panel we show the distribution of the stars at $t = 0.6$ Myr. Although the peak of the distribution is still at the position of the ionization front, there is a significant number of triggered stars inside of this radius. Therefore, the assumption of a triggered origin for the proplyds is definitely valid. The distribution shown here is the distribution of all triggered stars. For the proplyds, the distribution should be strongly cored and drop with radius as $R^{-2.58}$, as shown by Henney & Arthur (1998). As we are not investigating the interaction of the stellar feedback with the triggered stars, our model can not predict the distribution of the proplyds. A final test for this scenario are the proper motions of the triggered stars. In Figure 5 (right hand panel), we plot the radial velocity versus the radius. As expected, there is a strong correlation with distance. The further out

the stars are, the slower they are, whereas closer to the centre they move much faster, as their kinetic energy is close to maximal. In addition, some stars have positive radial velocity, they already had their closest encounter and are moving outwards. Thus, our conjecture could be conclusively proven by a detailed analysis of the proper motion of proplyds and triggered stars.

The parameters chosen for Orion are the combination of an older star and a lower density as inferred from from the outskirts of Orion. In general, several combinations of density and stellar age are possible, e.g. a younger star and a correspondingly denser medium, which would result in an earlier return time (cf §3). The return time and the assumed age of θ Orions C of 0.6 Myr is slightly larger than the estimated lifetime of the proplyds of about 0.5 Myr. However, if the stars return after spending most of their lifetime further away from the ionizing source (Figure 5), their life-time will be longer than the ones estimated from their current, higher photo-evaporation in close proximity. The age determination is a main uncertainty, e.g. Jeffries et al. (2011) adopt a higher age for the subgroup, but do not exclude a smaller age like the one adopted here (as suggested by e.g. Smith et al. 2005; Tobin et al. 2009). For our model, the challenge is to explain the fast return, a slower return, i.e. a higher age is not a problem. We therefore conclude, that the proplyds in Orion are indeed the smoking gun of a population of stars triggered in an ionization shell.

6 DISCUSSION & CONCLUSIONS

In general, the stars inside HII-regions are most likely not stars triggered within the shell of the ionization front, as they would have formed with too high radial velocities to have returned yet. However, in dense cases like Orion, the HII region confinement is strong enough to explain the observed proplyds by our model of ionization triggered star formation with a subsequent return.

The HII region expands rapidly and the in situ and triggered populations of stars will be mixed, especially after the reflection point (see §5), when triggered stars are moving inwards and outwards. Therefore, we do not expect an age spread proceeding with the speed of the ionization front. Instead, we propose a sequence which shows a radial dependence, and which results from different levels of harassment.

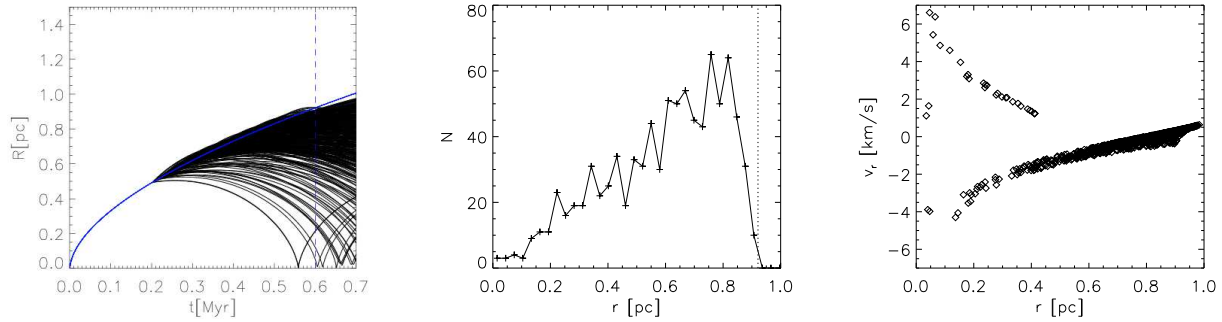


Figure 5. The special case of Orion: to explain the high current electron density we assume a high initial density, which in turn leads to the return of triggered stars. Left panel: trajectories of the particles (stars). Blue solid line: position of the ionization front, blue dashed line: current age of θ Orionis C. Middle panel: number of triggered stars in radial bins at $t=0.6$ Myr. Dashed line: current front position. Right hand panel: radial velocity versus radius at $t=0.6$ Myr. A clear correlation with distance can be seen. The stars with positive velocities already had the closest encounter and are moving outwards again

Closest in are the proplyds, where the disk of a young star interacts directly with the feedback of the massive star. In the medium range, there are Class II protostars, where the ionization already was able to remove the envelope partly. At the outskirts of the HII region, there are Class I stars, which either have been triggered by the ionizing radiation or pre-existed and have not lost their envelope yet, as the feedback is much weaker further away.

Whether the protostars together with the central mass form a bound or an unbound cluster depends on the precise initial conditions and has to be determined with e.g. N-Body simulations. The triggered stars here, however, are likely to be loosely bound or will be removed due to their high initial velocity. In addition, the spherically symmetrical potential gets diminished by the gas loss, so the tidal radius shrinks. Furthermore, as soon as the central stars explode in a supernova, additional gas is going to be removed, leading to an even shallower potential.

We have shown that a triggered population shows a different density distribution compared e.g. to a randomly formed distribution of stars. Especially, the triggered distribution shows a characteristic peak at the current position of the shock front. Inside the HII-region, the stellar component is dominated by in situ stars. For the densest regions like Orion, enough triggered stars return within 0.6 Myr to provide a feasible explanation for the origin of the proplyds as well as their exclusiveness.

7 ACKNOWLEDGEMENTS

We thank the referee for valuable comments on the manuscript. M.G. acknowledges funding by the Alexander von Humboldt Foundation in form of a Feodor-Lynen Fellowship. Part of A.B.'s research was supported by the Excellence Cluster "Origin and Structure of the Universe".

REFERENCES

Bally J., Licht D., Smith N., Walawender J., 2005, *AJ*, 129, 355
 Brown A. G. A., de Geus E. J., de Zeeuw P. T., 1994, *A&A*, 289, 101
 De Marco O., O'Dell C. R., Gelfond P., Rubin R. H., Glover S. C. O., 2006, *AJ*, 131, 2580

Donati J.-F., Babel J., Harries T. J., Howarth I. D., Petit P., Semel M., 2002, *MNRAS*, 333, 55
 Elmegreen B. G., Lada C. J., 1977, *ApJ*, 214, 725
 Ferland G. J., Korista K. T., Verner D. A., Ferguson J. W., Kingdon J. B., Verner E. M., 1998, *PASP*, 110, 761
 García-Arredondo F., Henney W. J., Arthur S. J., 2001, *ApJ*, 561, 830
 Gritschneider M., Naab T., Burkert A., Walch S., Heitsch F., Wetzstein M., 2009, *MNRAS*, 393, 21
 Henney W. J., Arthur S. J., 1998, *AJ*, 116, 322
 Henney W. J., Arthur S. J., de Colle F., Mellema G., 2009, *MNRAS*, 398, 157
 Henney W. J., O'Dell C. R., 1999, *AJ*, 118, 2350
 Hester J. J., Scowen P. A., Sankrit R., Lauer T. R., Ajhar E. A., Baum W. A., Code A., Currie D. G., Danielson G. E., Ewald S. P., Faber S. M., Grillmair C. J., Groth E. J., Holtzman J. A., Hunter D. A., Kristian J., Light R. M., Lynds C. R. e. a., 1996, *AJ*, 111, 2349
 Hillenbrand L. A., 1997, *AJ*, 113, 1733
 Howarth I. D., Prinja R. K., 1989, *ApJS*, 69, 527
 Jeffries R. D., Littlefair S. P., Naylor T., Mayne N. J., 2011, *MNRAS*, 418, 1948
 Laques P., Vidal J. L., 1979, *A&A*, 73, 97
 Meaburn J., 1988, *MNRAS*, 233, 791
 O'Dell C. R., 1998, *AJ*, 115, 263
 O'Dell C. R., Wen Z., Hu X., 1993, *ApJ*, 410, 696
 Rubin R. H., Simpson J. P., O'Dell C. R., McNabb I. A., Colgan S. W. J., Zhuge S. Y., Ferland G. J., Hidalgo S. A., 2011, *MNRAS*, 410, 1320
 Smith N., Bally J., Morse J. A., 2003, *ApJL*, 587, L105
 Smith N., Bally J., Shuping R. Y., Morris M., Kassis M., 2005, *AJ*, 130, 1763
 Spitzer L., 1978, *Physical processes in the interstellar medium*. Wiley-Interscience, New York
 Störzer H., Hollenbach D., 1999, *ApJ*, 515, 669
 Strömgren B., 1939, *ApJ*, 89, 526
 Tobin J. J., Hartmann L., Furesz G., Mateo M., Megeath S. T., 2009, *ApJ*, 697, 1103
 Wright N. J., Drake J. J., Drew J. E., Guarcello M. G., Gutermuth R. A., Hora J. L., Kraemer K. E., 2012, *ApJL*, 746, L21